Siva1 suppresses epithelial–mesenchymal transition and metastasis of tumor cells by inhibiting stathmin and stabilizing microtubules

Nan Li[a], Peng Jiang[b], Wenjing Du[b], Zhengsheng Wu[c], Cong Li[a], Mengran Qiao[a], Xiaolu Yang[b,1], and Mian Wu[a,1]

[a]Hefei National Laboratory for Physical Sciences at Microscale and School of Life Sciences, University of Science and Technology of China, Hefei, Anhui 230027, China; [b]Department of Cancer Biology and Abramson Family Cancer Research Institute, University of Pennsylvania School of Medicine, Philadelphia, PA 19104; and [c]Department of pathology, Anhui Medical University, Hefei, Anhui 230032, China

Edited by Joan S. Brugge, Harvard Medical School, Boston, MA, and approved June 20, 2011 (received for review November 19, 2010)

Epithelial–mesenchymal transition (EMT) enables epithelial cells to acquire motility and invasiveness that are characteristic of mesenchymal cells. It plays an important role in development and tumor cell metastasis. However, the mechanisms of EMT and their dysfunction in cancer cells are still not well understood. Here we report that Siva1 interacts with stathmin, a microtubule destabilizer. Siva1 inhibits stathmin's activity directly as well as indirectly through Ca^{2+}/calmodulin-dependent protein kinase II-mediated phosphorylation of stathmin at Ser16. Via the inhibition of stathmin, Siva1 enhances the formation of microtubules and impedes focal adhesion assembly, cell migration, and EMT. Low levels of Siva1 and Ser16-phosphorylated stathmin correlate with high metastatic states of human breast cancer cells. In mouse models, knockdown of Siva1 promotes cancer dissemination, whereas overexpression of Siva1 inhibits it. These results suggest that microtubule dynamics are critical for EMT. Furthermore, they reveal an important role for Siva1 in suppressing cell migration and EMT and indicate that down-regulation of Siva1 may contribute to tumor cell metastasis.

CaMKII | cell motility | tumor metastasis

The spread of cancer cells from a primary tumor to distant organs causes the vast majority of deaths from cancer, yet this process is still poorly understood (1). For carcinomas, which originate from epithelial cells and account for most tumors, acquisition of invasiveness and motility requires them to undergo a dramatic transition to a mesenchymal state (epithelial–mesenchymal transition or EMT) (2, 3). EMT involves the cooperation between genetic alterations in tumor cells and signals released by the tumor microenvironment, with the subsequent reactivation of EMT-promoting transcriptional factors that normally function during early embryogenesis and during wound healing. These transcriptional regulators suppress the expression of epithelial proteins, including the transmembrane protein E-cadherin, which maintains epithelial cell–cell contact and induces the expression of mesenchymal proteins such as vimentin, an intermediate filament component of the mesenchymal cell cytoskeleton. The changes in gene expression cause disruption of intercellular adhesion, loss of apicobasal polarity, and dynamic reorganization of the cytoskeleton, which leads to enhancement of cell motility.

Cell motility is driven by dynamics of actin filament with the cooperation of microtubules. Although the role of actin cytoskeleton in EMT is well established, the role for microtubules has only recently begun to be elucidated (4–6). Microtubules are polymers of α/β-tubulin dimers. A notable factor that regulates microtubule dynamics is stathmin, which depolymerizes microtubules through both the sequestration of α/β-tubulin heterodimers and the enhancement of microtubule catastrophe (7–9). Deficiency in stathmin impairs cell migration (10–12). Stathmin is inhibited by phosphorylation at its N-terminal region including Ser16 and Ser63 (13, 14). The contribution of stathmin to EMT is still not clear, nor is the regulation of stathmin phosphorylation well understood. In this study, we find that stathmin interacts with Siva1, a molecule involved in aspects of apoptosis regulation (15–18). Our study reveals a critical role for stathmin and microtubule dynamics in promoting EMT. We further show that Siva1 is an important negative regular of stathmin and that the down-regulation of Siva1 may promote EMT and tumor cell dissemination.

Results

Siva1 Interacts with Stathmin. Our recent study revealed a role for Siva1 in regulating p53 (18). To better understand the function of Siva1, we performed a yeast two-hybrid screen using Siva1 as the bait and identified stathmin as a Siva1-interacting protein. Using reciprocal immunoprecipitation assays, endogenous Siva1 and stathmin were found to interact with each other in human osteosarcoma U2OS cells (Fig. 1*A* and Fig. S1*A*). Similarly, the interactions between endogenous Siva1 and stathmin were observed in two human breast cell lines, HBL-100 and MCF-7 (Fig. S1 *B* and *C*). Stathmin is a cytoplasmic protein, whereas Siva1 resides in both the cytoplasm and the nucleus. As expected, the Siva1–stathmin interaction occurred mainly in the cytoplasm (Fig. 1*B*). Furthermore, in an in vitro pull-down assay using purified proteins, 6xHis-tagged stathmin (His-stathmin) bound to a GST fusion of Siva1, but not GST alone (Fig. S1*D*), indicating that Siva1 and stathmin directly associate with each other.

To delineate the regions in Siva1 and stathmin that mediate their interaction, we generated a panel of mutants of both proteins, each fused to the enhanced GFP (Fig. S1 *E* and *G*). Siva1 deletion mutants containing the C-terminal region (ΔN, ΔDDHR, and C), but not a mutation lacking this region (ΔC), interacted with stathmin (Fig. S1*F*). In contrast, stathmin deletion mutants containing the N-terminal region (NC, NM, and N), but not a mutant lacking it (MC), interacted with Siva1 (Fig. S1*H*). Thus, the Siva1 C-terminal region and the stathmin N-terminal region mediate the interaction between these two proteins.

Siva1 Attenuates Stathmin's Microtubule-Destabilizing Activity. To investigate the functional consequence of the Siva1–stathmin interaction, we first evaluated the effect of Siva1 on the association of stathmin with tubulin. As shown in Fig. 1*C*, increasing Siva1 expression through transient transfection reduced the interaction between endogenous stathmin and α-tubulin. In contrast, Siva1ΔC, which was unable to bind to stathmin (Fig. S1*F*),

Author contributions: N.L., P.J., W.D., X.Y., and M.W. designed research; N.L., P.J., W.D., Z.W., C.L., and M.Q. performed research; N.L., P.J., W.D., X.Y., and M.W. analyzed data; and N.L., X.Y., and M.W. wrote the paper.

The authors declare no conflict of interest.

This article is a PNAS Direct Submission.

[1]To whom correspondence may be addressed. E-mail: xyang@mail.med.upenn.edu or wumian@ustc.edu.cn.

This article contains supporting information online at www.pnas.org/lookup/suppl/doi:10.1073/pnas.1017372108/-/DCSupplemental.

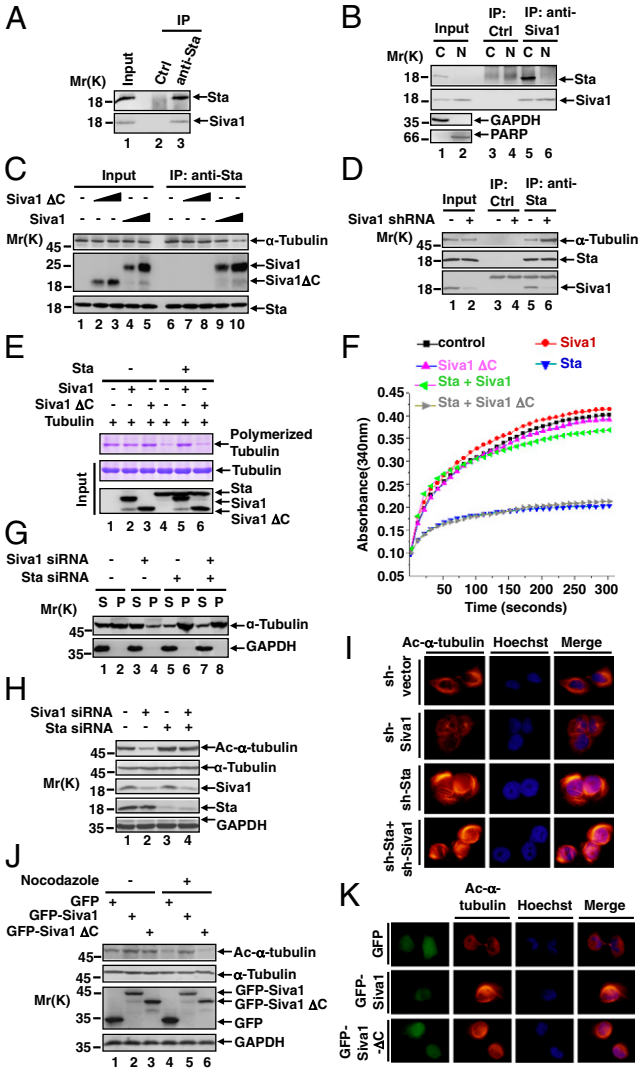

Fig. 1. Siva1 binds to and inhibits stathmin, promoting the formation of microtubules. (*A*) U2OS cell lysates were incubated with anti-stathmin (Sta) or a control antibody. The input and immunoprecipitated (IP) proteins were analyzed by Western blot. Molecular weight standards (M_r, in kilodalton) are shown on the left. (*B*) U2OS cell lysates were separated into cytosolic (C) and nuclear (N) fractions. Each fraction was subject to immunoprecipitation with either anti-Siva1 or control antibody, followed by Western blot. GAPDH and PARP were analyzed as controls for cytosolic and nuclear fractions, respectively. (*C*) U2OS cells were transiently transfected without or with increasing amounts of Flag-Siva1 or Flag-Siva1ΔC. Cell lysates were immunoprecipitated with anti-stathmin antibody, followed by Western blot analysis. (*D*) Lysates of U2OS cells stably expressing control shRNA (–) or Siva1 shRNA were analyzed by immunoprecipitation and Western blot. (*E*) Purified Flag-tagged proteins were incubated with tubulins. Polymerized (*Top*) and input (*Middle*) tubulin proteins were analyzed by Coomassie blue staining, and input Flag-tagged proteins (*Bottom*) by Western blot. (*F*) Tubulin polymerization in the presence of stathmin, Siva1, and Siva1 ΔC in the indicated combination. (*G*) U2OS cells were transfected with or without Siva1 siRNA and/or stathmin siRNA. Supernatant (S) and pellet (P) fractions of the cell lysates were analyzed. (*H*) Lysates of U2OS cells transfected with the indicated siRNA were analyzed by Western blot. (*I*) U2OS cells stably expressing the indicated shRNA were stained with Hoechst and rhodamine-conjugated anti-ac-α-tubulin antibody. (*J*) U2OS cells transfected with GFP, GFP-Siva1, or GFP-Siva1 ΔC were treated with or without nocodazole (20 μM). (*K*) U2OS cells transfected with GFP, GFP-Siva1, or GFP-Siva1 ΔC were stained with Hoechst and hodamine-conjugated anti-ac-α-tubulin antibody.

exhibited no such effect. Conversely, knockdown of endogenous Siva1 with shRNA strongly increased the stathmin–α-tubulin interaction (Fig. 1*D*). These results show that Siva1 inhibits stathmin from interacting with α-tubulin.

We next investigated whether Siva1 counteracts stathmin's ability to destabilize microtubules. Purified tubulins polymerized in vitro, as shown by a sedimentation assay (Fig. 1*E*). When stathmin was incubated with tubulins, it markedly reduced the formation of the tubulin polymer, as expected (Fig. 1*E*). However, when added along with stathmin, Siva1, but not Siva1 ΔC, effectively neutralized the inhibitory effect of stathmin (Fig. 1*E*). We also assayed tubulin polymerization on the basis of the increase of absorbance over time (Fig. 1*F*). Again, Siva1, but not Siva1 ΔC, strongly negated the inhibitory effect of stathmin and almost completely restored tubulin polymerization that was reduced by stathmin. In the absence of stathmin, Siva1 exhibited no or minimal effect on tubulin polymerization (Fig. 1 *E* and *F*).

We next examined the effect of Siva1 on microtubules in vivo. siRNA-mediated knockdown of Siva1 disrupted microtubules (Fig. 1*G*). This effect of Siva1 was dependent on stathmin; when stathmin was knocked down, ablation of Siva1 could no longer affect the microtubules. We also assessed the effect of Siva1 on the levels of acetylated α-tubulin, which is present only in polymerized tubulin (19, 20). As shown by Western blot and immunostaining analyses, silencing of Siva1 strongly reduced the levels of acetyl-α-tubulin in U2OS cells (Fig. 1 *H* and *I*). The effect of Siva1 on acetyl-α-tubulin was also dependent on stathmin (Fig. 1*H*). In contrast, overexpression of Siva1, but not Siva1 ΔC, elevated the levels of acetyl-α-tubulin in U2OS cells (Fig. 1 *J* and *K*). Furthermore, Siva1 protected microtubules from nocodazole-induced depolymerization, whereas Siva1 ΔC provided no such protection (Fig. 1*J*). Together these data indicate that Siva1 stabilizes microtubules through inhibiting stathmin.

Siva1 Promotes Phosphorylation of Stathmin at Ser16 via CaMK II. Previous studies showed that phosphorylation in the N-terminal region, particularly at Ser16 and Ser63, decreases stathmin's activity (8, 9). This prompted us to investigate whether, in addition to direct inhibition of stathmin, Siva1 regulates stathmin phosphorylation. An increase in the levels of Siva1 led to concomitant increase in stathmin phosphorylation at Ser16 (pS16-stathmin), but not at Ser63 (Fig. 2*A*), whereas knockdown of Siva1 by shRNA markedly decreased the level of pS16-stathmin (Fig. 2*B*). Stathmin is phosphorylated at Ser16 by cAMP-dependent kinase (PKA) and calmodulin-dependent kinase (CaMK, both isoforms II and IV) (13, 21, 22). When cells were treated with EGTA, which chelates calcium and thus diminishes the activity of CaMK, stathmin phosphorylation at Ser16 decreased (Fig. 2*C*). Under this condition, knockdown of Siva1 no longer affected stathmin phosphorylation, suggesting that one or both CaMK isoforms might be involved in Siva1-induced stathmin phosphorylation. When CaMK II, but not when CaMK IV, was ablated by siRNA, the effect of Siva1 on stathmin phosphorylation diminished (Fig. 2*D*). Similar results were observed when cells were treated with AIP II, a specific inhibitor for CaMK II (Fig. 2*E*). Together, these results suggest that Siva1 promotes Ser16 phosphorylation of stathmin by CaMK II.

To investigate the mechanism by which Siva1 stimulates stathmin phosphorylation, we tested whether it associates with CaMK II. An immunoprecipitation assay showed that endogenous CaMK II interacted with GFP-Siva1, but not with GFP (Fig. S2). Using a panel of Siva1 mutants revealed that the N-terminal region of Siva1 interacts with CaMKII (Fig. S2). Because Siva1 binds to stathmin through the C terminus (Fig. S1*F*), we tested whether Siva1 simultaneously binds to both stathmin and CaMK II. The interaction between endogenous stathmin and CaMK II was enhanced when Siva1 levels were elevated (Fig. 2*F*) and was reduced when Siva1 was knocked down (Fig. 2*G*).

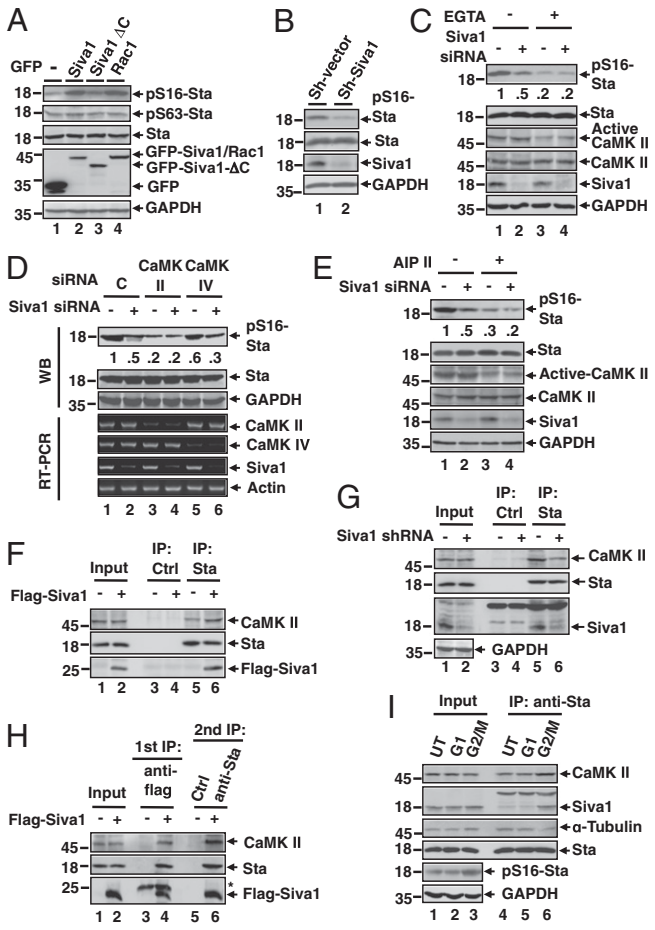

Fig. 2. Siva1 enhances CaMK II-mediated phosphorylation of stathmin at Ser16. (*A*) U2OS transfected with GFP (–) or the indicated GFP fusion were analyzed for protein expression and stathmin phosphorylation at Ser16 (pS16) and Ser63 (pS63). Rac1, a kinase for Ser16 (36), was included as a positive control. (*B*) U2OS cells stably expressing control (C) or Siva1 shRNA for protein expression and Ser16 phosphorylation. (*C*) U2OS cells transfected with control siRNA or Siva1 siRNA were treated with or without EGTA (5 mM) for 2 h. The relative pS16-stathmin/stathmin ratios are indicated. (*D*) U2OS cells transfected with the indicated siRNA were analyzed for protein expression by Western blot (WB, *Upper*) and for gene transcripts by RT-PCR (*Lower*). The relative pS16-stathmin/stathmin ratios are indicated. (*E*) U2OS cells transfected with control siRNA (–) or Siva1 siRNA were treated with or without 10 μM AIP II for 4 h. (*F* and *G*) Lysates of U2OS cells transfected with control vector or Flag-Siva1 (*F*) or lysates of U2OS cells stably expressing control shRNA or Siva1 shRNA (*G*) were immunoprecipitated with anti-stathmin antibody or control antibody. (*H*) U2OS cells were transfected with control vector or Flag-Siva1. Cell lysates were immunoprecipitated with anti-Flag antibody. Flag-Siva1 and the associated proteins were eluted with 3xFlag peptide. Ten percent of the eluent was saved for Western blot, and the remaining eluent was used for secondary immunoprecipitation assay with anti-stathmin or control antibody. Asterisk indicates IgG light chain. (*I*) U2OS cells were untreated (UT), arrested at G1 phase by serum deprivation, or arrested at G2/M phase by treating with nocodazole (10 μM, 4 h). Lysates were analyzed by immunoprecipitation and Western blot.

These results suggest that Siva1 mediates the interaction between CaMK II and stathmin. Furthermore, a two-step immunoprecipitation assay confirmed the existence of a ternary complex comprising Siva1, stathmin, and CaMK II (Fig. 2*H*).

The phosphorylation of stathmin varies during the cell cycle and reaches its maximum when cells enter mitosis (23) (Fig. 2*I*, lanes 3 vs. 2). Of note, at the G2/M phase, both the stathmin–Siva1 and the stathmin–CaMKII interactions increased, but the stathmin–α-tubulin interaction decreased (lanes 5 vs. 6). These results suggest that the increase in stathmin phosphorylation at the G2/M phase is due to the formation of the ternary Siva1–stathmin–CaMK II complex, which consequently weakens the stathmin–α-tubulin interaction. The inactivation of stathmin at the G2/M phase of cell cycle may enhance the formation of microtubules, enabling the proper progression of mitosis.

Siva1 Suppresses EMT and Cell Migration via Stathmin. To evaluate the role of Siva1 in cell migration, we performed both wound-healing and transwell migration assays. Up-regulation of Siva1 strongly inhibited directional cell migration toward a "wound" in a cell monolayer (Fig. 3*A*), whereas knockdown of Siva1 significantly enhanced it (Fig. 3*B*). Up-regulation of Siva1 also markedly inhibited cell migration through a permeable filter (Fig. 3*C*), whereas knockdown of Siva1 increased the migration (Fig. 3*D*). However, when stathmin was silenced, the effect of Siva1 on cell migratory behavior was abrogated (Fig. 3*D*). Therefore, Siva1 decreases cell migration through inhibiting stathmin.

The role of Siva1 in microtubule dynamics and cell migration prompted us to examine its role in EMT. Over-expression of Siva1, but not Siva1 ΔC, augmented the expression of epithelial markers (e.g., E-cadherin and α-catenin) and reduced the expression of mesenchymal markers (e.g., vimentin and fibronectin) in both MDA-MB-231 (mesenchymal-like) and U2OS (epithelial-like) cells (Fig. 3*E* and Fig. S3*A*). Knockdown of endogenous Siva1 had an opposite effect on the expression of these proteins in HBL-100, U2OS, and MCF-10A cells, as judged by both Western blot and immunofluorescence analyses (Fig. 3 *F* and *G* and Fig. S3 *B* and *C*). In contrast, knockdown of stathmin increased expression of epithelial markers and decreased expression of mesenchymal markers (Fig. 3*H* and Fig. S3*D*). Moreover, when stathmin was depleted, the effect of Siva1 on EMT diminished (Fig. 3*H* and Fig. S3*D*). These observations suggest that Siva1 counteracts the stimulatory effect of stathmin on mesenchymal phenotypes and underscore the importance of microtubule dynamics in EMT.

Previous studies showed that focal adhesion kinase (FAK) promotes EMT, tumor cell migration, and metastasis, whereas microtubules inhibit FAK and focal adhesion assembly (24). To further investigate the mechanism by which Siva1 and stathmin regulate cell migration and EMT, we examined their effects on the levels of Tyr397-phosphorylated focal adhesion kinase (pY397-FAK), a marker for focal adhesion assembly. Consistent with previous reports, nocodazole-mediated disruption of microtubules led to an elevation in the levels of pY397-FAK and a concurrent reduction in the level of E-cadherin and Ac-α-tubulin (Fig. 3*I*, lanes 1 vs. 2). These changes were reversed after cells were returned to nocodazole-free medium (lanes 3 and 4). Over-expression of Siva1 decreased the levels of pY397-FAK (Fig. 3*E*), whereas knockdown of Siva1 increased it (Fig. 3 *F* and *H*). Stathmin had an opposite effect on the level of pY397-FAK (Fig. 3*H*). Therefore, Siva1 may disrupt focal adhesion and enforce epithelial phenotypes through the stabilization of microtubules.

Down-Regulation of Siva1 and Ser16-Phosphorylated Stathmin in Human Breast Tumors. To investigate the role of Siva1 in tumor cell metastasis, we analyzed the expression of Siva1 and the level of pS16-stathmin in different breast cancer cell lines. Compared with untransformed breast cell lines or low metastatic breast tumor cell lines, both Siva1 and pS16-stathmin were notably down-regulated in high metastatic breast tumor cell lines (MDA-MB-468 and MDA-MB-231) (Fig. 4 *A* and *B*). To confirm this observation, we analyzed primary breast tumors, metastatic breast tumors, and the adjacent normal tissues (13–15 samples each). Normal breast tissues displayed relatively high levels of Siva1 and pS16-stathmin. In comparison, the primary and metastatic breast tumors exhibited progressively less Siva1 and pS16-

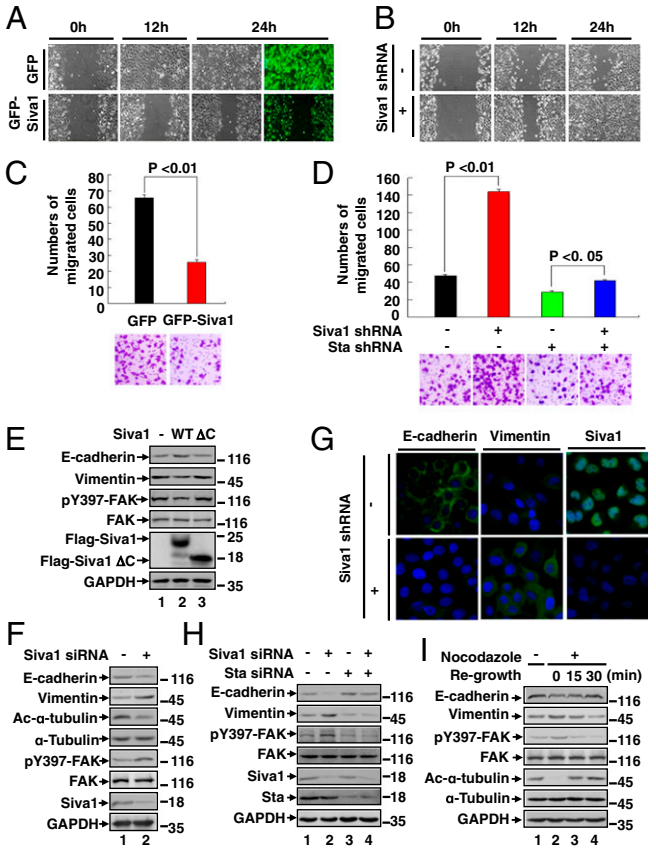

Fig. 3. Siva1 inhibits EMT and cell migration. (*A–D*) Effects of Siva1 overexpression (*A* and *C*) and depletion (*B* and *D*) on the migration of cultured U2OS were examined by wound-healing (*A* and *B*) and Matrigel migration (*C* and *D*) assays. Results are representative of three independent experiments. In *C* and *D*, migrated cells were plotted as the average number of cells per field of view. (*E*) Lysates of MDA-MB-231 cells transfected with control vector (–), Flag-Siva1, or Flag-Siva1 ΔC were analyzed for the expression of epithelial and mesenchymal markers and for the phosphorylation of FAK at Tyr397. (*F* and *G*) The expression levels of epithelial and mesenchymal markers were compared among HBL-100 cells transiently transfected with Siva1 siRNA or control siRNA using Western blot (*F*) and among HBL-100 cells stably transfected with Siva1 shRNA or the control vector using immunostaining (*G*). (*H* and *I*) HBL-100 cells were transfected with the indicated siRNAs (*H*) or treated with or without nocodazole (10 μM) for 4 h and then regrown in nocodazole-free medium for the indicated durations to allow for the formation of microtubules (*I*).

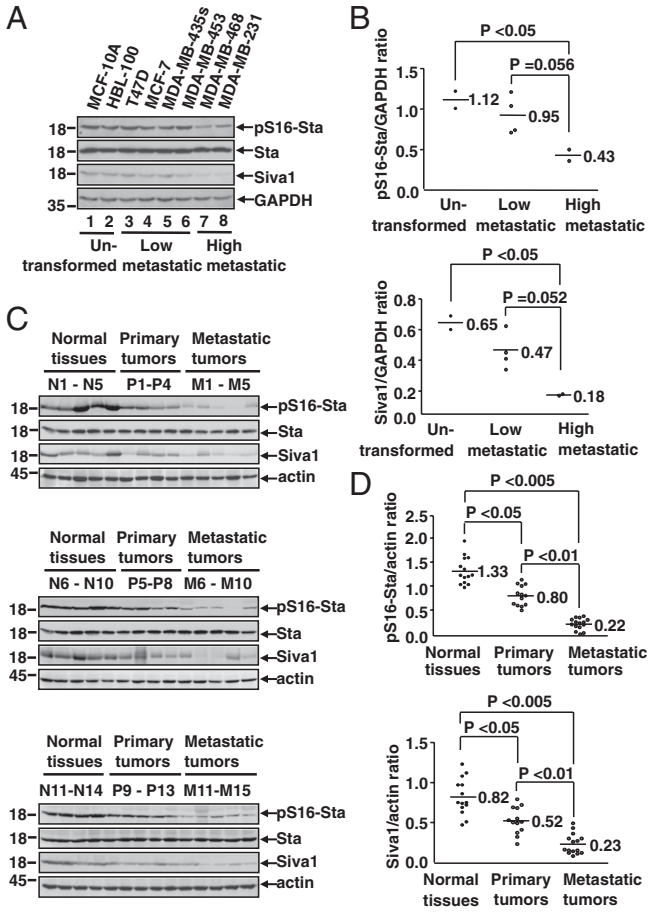

Fig. 4. Down-regulation of Siva1 and pS16-stathmin correlates with human breast tumor progression. (*A* and *B*) Western blot (*A*) and Graphpad prism analyses (*B*) of Siva1 and pS16-stathmin levels in eight different untransformed human breast cell lines and human breast cancer cell lines with low or high potentials for metastasis. (*C* and *D*) Siva1 expression and pS16-stathmin levels in normal breast tissues (n = 14), primary breast tumors (n = 13), and metastatic breast tumors (n = 15) were analyzed by Western blot (*C*) and Graphpad prism (*D*).

stathmin (Fig. 4 *C* and *D*). Therefore, low levels of Siva1 and pS16-stathmin correlate with the progression and metastasis of human breast tumors.

Siva1 Inhibits Breast Cancer Metastasis. To assess the role of Siva1 in tumor cell metastasis, we used xenograft models of metastasis. MCF7 cell lines stably expressing Siva1 shRNA or control shRNA were injected into nude mice via tail vein. The formation of the tumors in whole animals and in livers and lungs were examined by D-luciferin-based bioluminescence. As shown in Fig. 5*A*, mice injected with MCF7-Siva1 shRNA cells exhibited markedly increased tumor metastasis compared to mice injected with MCF7-control shRNA cells. Analysis of tumors in lungs and livers further verified the highly enhanced metastatic potential of MCF7-Siva1 shRNA cells. To test the generality of Siva1's effect on tumor metastasis, we generated B16-F10 mouse melanoma cells stably expressing GFP or GFP-Siva1. B16-F10 cells expressing GFP-Siva1 exhibited strongly reduced metastasis in the xenograft mouse models compared with B16-F10 cells expressing only GFP (Fig. 5 *B* and *C*). Taken together, these data demonstrate that Siva1 plays an important role in suppressing tumor metastasis.

Discussion

In this study we demonstrate that Siva1 counteracts stathmin, an important regulator for microtubule dynamics (7, 9), and define a role for Siva1 in the suppression of EMT and tumor metastasis (Fig. 5*D*). The activity of stathmin can be modulated minimally at two levels: its association with the α/β-tubulin heterodimers and its phosphorylation status. Siva1 acts at both levels: it strongly weakens the interaction between stathmin and tubulin (Fig. 1) and also promotes the interaction between stathmin and CaMK II (Fig. 2). The relative importance of these two functions in Siva1's ability to increase MT stability remains to be determined. Nevertheless, inhibition of stathmin by Siva1 leads to the stabilization of microtubule network and inhibition of cell migration.

Microtubules disruption facilitates the assembly of focal adhesions and enhances cell migration (25–28). Our results illustrate that through regulating microtubule dynamics, stathmin promotes EMT, whereas Siva1 inhibits it. These results provide support for the role of microtubules in suppressing EMT in tumor cells. Besides regulating cell migration and EMT, the Siva1–CaMKII–

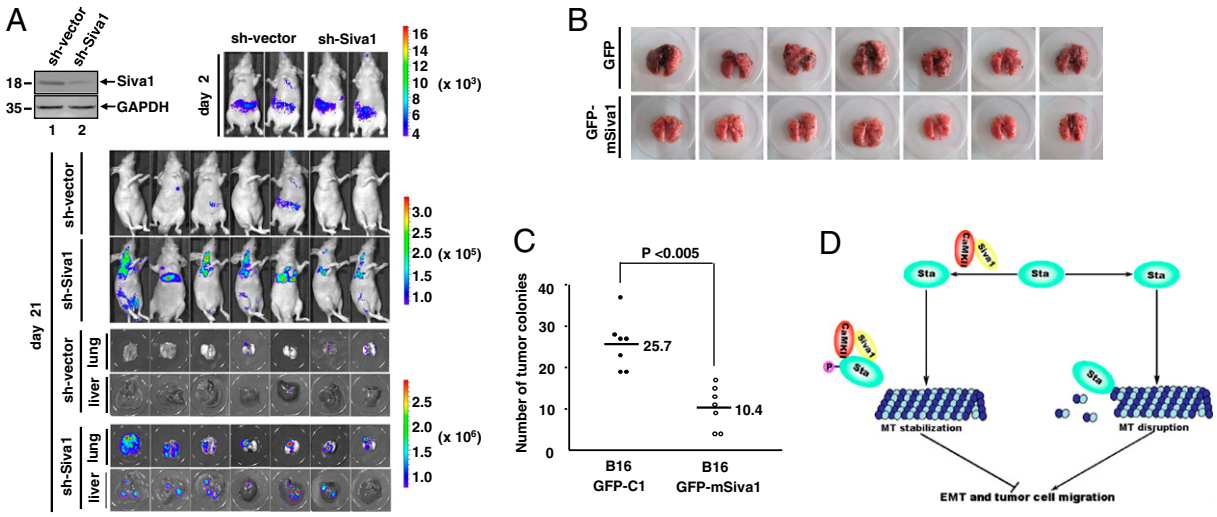

Fig. 5. Siva1 suppresses metastasis of breast cancer cells. (*A*) MCF7 cells stably expressing control shRNA or Siva1 shRNA (each also expressing luciferase) were injected into nude mice. Tumors in whole animals and in lungs and livers were monitored by bioluminescence imaging. The expression of Siva1 in MCF7 cells is shown at *Upper Left*. (*B* and *C*) B16-F10 cells stably expressing GFP or GFP-Siva1 were injected into nude mice. Formation of tumors in lungs was analyzed (*B*), and numbers of tumors are shown (*C*). (*D*) A model for the role of Siva1 in the stathmin-mediated microtubule disassembly and EMT.

sthathmin axis may also function at mitosis to enhance microtubule assembly needed for chromosome movement (Fig. 2*I*).

In some human cancer types including sarcomas, non–small-cell lung cancers, and Wilms tumors, up-regulation of stathmin has been linked to more aggressive phenotypes with high invasion and metastasis (8, 10, 29, 30). However, the metastatic and noncancerous breast tumor tissues examined in this study showed no noticeable difference in the level of stathmin. Instead, both the levels of Siva1 and pS16-stathmin are much lower in highly metastatic breast tumors compared with normal or low metastatic breast tumors (Fig. 4). This observation provides insight into stathmin's function in cancer progression and indicates that the decrease in Siva1 and pS16-stathmin may contribute to metastasis of human breast cancer. Siva1 and stathmin may be biomarkers and therapeutic targets for breast cancer.

Methods

Reagents and Antibodies. The antibodies against the following proteins, tags, and phosphorylated/acetylated proteins were purchased from the indicated sources: GAPDH, 6xHis tag, active CaMK II, and pS16-stathmin (Cell Signaling); actin, stathmin, α-tubulin, Ac-α-tubulin (Abcam); Siva1 (for immunoprecipitation and immunostaining), pS16-stathmin, pS63-stathmin, FAK, pY397-FAK, and CaMK IIα (Santa Cruz Biotechnology); GFP, E-cadherin, α-catenin, and Fibronectin (BD Bioscience); vimentin (Thermo Scientific); poly ADP-ribose polymerase (PARP) (Upstate Biotechnology); Flag (Sigma and Abmart); and Siva1 (for Western blot) (Abnova). Hoechst, Taxol, and nocodazole were purchased from Sigma-Aldrich; G418, puromycin and autocamtide-2-related inhibitory peptide II (AIP II) from Calbiochem; and D-luciferin from Gold Biotechnology.

Plasmids and Protein Purification. Rac1, Siva1, and Siva1 deletion fragments were amplified from a human fetal brain cDNA library (Clontech). Stathmin and stathmin deletions were amplified from Myc-stathmin (gifts from Prof. Xinmin Cao, Institute of Molecular and Cell Biology, Singapore). For mammalian expression, the plasmids were cloned into pEGFP-C1 (Clontech) or pcDNA3 Flag vectors (Invitrogen). GST-Siva1 was constructed in pGEX-5X-3, and 6xHis-stathmin in pET-21a(+) (Novagen), and these proteins were purified using glutathione beads and Ni-NTA beads, respectively. Porcine brain tubulin was purified by two warm/cold polymerization cycles followed by phosphocellulose chromatography (GE Healthcare HiTrap SP HP) as previously described (31, 32).

Yeast Two-Hybrid Assay. Human Siva1 cloned into the pGBK-T7 plasmid was used as bait in a yeast two-hybrid screen of a fetal brain cDNA library (Clontech). Positive clones were confirmed by an X-gal filter assay and sequenced.

Cell Culture, Transfection, siRNA, and Stable Cell Lines. Cell lines were cultured in DMEM containing 10% FBS and transfected using Lipofectamine 2000 (Invitrogen). siRNAs against human Siva1, stathmin, CaMK, and CaMK IV were purchased from Santa Cruz Biotechnology. shRNAs against Siva1 and stathmin were constructed with the pSUPER shRNA system (Clontech) and used for the establishment of stable cell lines. The targeted sequences are 5′-cagtgacatgtacgagaaa-3′ (Siva1) and 5′-aggcaatagaagagaacaa-3′ (stathmin). MCF7-control shRNA and MCF7 Siva1-shRNA stable cells expressing luciferase were prepared using the pLentiLox 3.7 lentiviral system.

Subcellular Fractionation, Immunoprecipitation, GST Pull-down, and Western Blot. Subcellular fractionation, immunoprecipitation, GST pull-down, and Western Blot were performed as described previously (18, 33).

Immunofluorescence. Cells cultured in 24-well chamber slides or on coverslips were washed twice with cold 1× PBS, fixed with 4% paraformaldehyde for 10 min, permeabilized with 0.1% Triton X-100 for 5 min (except for staining the cell membrane-bound E-cadherin), blocked with 5% BSA, and incubated first with indicated antibodies and followed by a rhodamine-conjugated anti-mouse IgG antibody. The cells were then mounted with Hoechst 33342 reagent (Sigma) for nuclear staining, and the images were acquired with an Olympus DP71X microscope.

In Vitro Tubulin Polymerization. The in vitro assay of polymerized tubulin was performed as previously described (34). Flag-tagged proteins expressed in 293T cells were affinity purified with EZview Red Anti-Flag M2 Affinity Gel (Sigma) and eluted with 3xFlag peptide. Purified Flag-tagged proteins were mixed with α/β-tubulins purified from porcine brain (Sigma) in tubulin assembly buffer [80 mM Pipes (pH 6.8), 0.5 mM EGTA, 2 mM $MgCl_2$, 1 mM GTP, 1 mM ATP, and 10% glycerol] and incubated at 37 °C for 1h. Polymerized tubulin was collected by centrifugation (15,000 × g for 30 min). Alternatively, porcine tubulin (20 μM) was mixed with indicated proteins in tubulin assembly buffer at 37 °C, and tubulin polymerization was observed by measuring the absorbance of the solution at 340 nm.

In Vivo Polymerized Tubulin Assay. The in vivo assay of polymerized tubulin was performed as previously described (35). Briefly, cells were lyzed in microtubule-stabilizing buffer [0.1 M Pipes (pH 6.9), 2 M glycerol, 5 mM $MgCl_2$, 2 mM EGTA, and 0.5% Triton X-100] supplemented with 4 μM Taxol to maintain microtubule stability during isolation. Lysates were centrifugated, and microtubles in the pellet were subjected to Western blot analysis.

Cell Migration Assays. Cells seeded in six-well plates were serum starved for 12 h. A linear wound was created using a pipette tip. Wounds were then observed at various times. Alternatively, cells were serum starved for 24 h, plated into the top side polycarbonate Transwell filter chambers coated with

Matrigel (BD BioCoat Invasion Chamber), and cultured for 8 h. Migratory cells on the lower membrane surface were fixed in 1% paraformaldehyde, stained with crystal violet, and counted (10 random 40× fields per well). Cell counts are expressed as the average number of cells per field of view. Three independent experiments were performed.

Tissue Samples. Specimens from 13 cases of primary breast cancer tissue, 15 cases of metastatic breast cancer tissue, and 14 cases of noncancerous breast tissue were collected from the Department of Pathology, Anhui Medical University (Hefei, China).

In Vivo Metastasis Assay. MCF and B16-F10 stable cell lines (1×10^6) were injected into 6-wk-old Balb/C nude mice via tail vein, and tumor formation and metastasis were analyzed 3 wk later. For MCF7 cell lines, mice were injected with D-luciferin and were imaged for 5 min on the IVIS200 (Caliper LS) imaging systems. To evaluate tumor metastasis into lungs and livers, mice were killed, and organs were incubated with D-luciferin for 15 min and imaged. Quantification was performed by LivingImage 2.6 software. For B16-F10 cell lines, the lungs from injected mice were dissected and imaged and the tumor colonies counted.

ACKNOWLEDGMENTS. We thank Prof. Xinmin Cao for providing us with myc-stathmin construct and Prof. Tao Zhu for the breast cancer cell lines. This work was supported by National Natural Science Foundation of China Grants 31030046 and 30871290 (to M.W.) and 30728003 (to X.Y.), Ministry of Science and Technology of China Grants 2010CB912804 and 2011CB966302 (to M.W.), Chinese Academy of Sciences Grant XDA01020104 (to M.W.), and US National Institutes of Health Grant CA088868 and Department of Defense Grant W81XWH-07-1-0336 (to X.Y.).

1. Chambers AF, Groom AC, MacDonald IC (2002) Dissemination and growth of cancer cells in metastatic sites. *Nat Rev Cancer* 2:563–572.
2. Polyak K, Weinberg RA (2009) Transitions between epithelial and mesenchymal states: Acquisition of malignant and stem cell traits. *Nat Rev Cancer* 9:265–273.
3. Thiery JP, Acloque H, Huang RY, Nieto MA (2009) Epithelial-mesenchymal transitions in development and disease. *Cell* 139:871–890.
4. Rodriguez OC, et al. (2003) Conserved microtubule-actin interactions in cell movement and morphogenesis. *Nat Cell Biol* 5:599–609.
5. Small JV, Geiger B, Kaverina I, Bershadsky A (2002) How do microtubules guide migrating cells? *Nat Rev Mol Cell Biol* 3:957–964.
6. Nakaya Y, Sukowati EW, Wu Y, Sheng G (2008) RhoA and microtubule dynamics control cell-basement membrane interaction in EMT during gastrulation. *Nat Cell Biol* 10:765–775.
7. Belmont LD, Mitchison TJ (1996) Identification of a protein that interacts with tubulin dimers and increases the catastrophe rate of microtubules. *Cell* 84:623–631.
8. Curmi PA, et al. (1999) Stathmin and its phosphoprotein family: General properties, biochemical and functional interaction with tubulin. *Cell Struct Funct* 24:345–357.
9. Cassimeris L (2002) The oncoprotein 18/stathmin family of microtubule destabilizers. *Curr Opin Cell Biol* 14:18–24.
10. Baldassarre G, et al. (2005) p27(Kip1)-stathmin interaction influences sarcoma cell migration and invasion. *Cancer Cell* 7:51–63.
11. Giampietro C, et al. (2005) Stathmin expression modulates migratory properties of GN-11 neurons in vitro. *Endocrinology* 146:1825–1834.
12. Jin K, et al. (2004) Proteomic and immunochemical characterization of a role for stathmin in adult neurogenesis. *FASEB J* 18:287–299.
13. Marklund U, et al. (1994) Serine 16 of oncoprotein 18 is a major cytosolic target for the Ca2+/calmodulin-dependent kinase-Gr. *Eur J Biochem* 225:53–60.
14. Lawler S (1998) Microtubule dynamics: If you need a shrink try stathmin/Op18. *Curr Biol* 8:R212–R214.
15. Prasad KV, et al. (1997) CD27, a member of the tumor necrosis factor receptor family, induces apoptosis and binds to Siva, a proapoptotic protein. *Proc Natl Acad Sci USA* 94:6346–6351.
16. Xue L, et al. (2002) Siva-1 binds to and inhibits BCL-X(L)-mediated protection against UV radiation-induced apoptosis. *Proc Natl Acad Sci USA* 99:6925–6930.
17. Chu F, et al. (2005) Expression of Siva-1 protein or its putative amphipathic helical region enhances cisplatin-induced apoptosis in breast cancer cells: Effect of elevated levels of BCL-2. *Cancer Res* 65:5301–5309.
18. Du W, et al. (2009) Suppression of p53 activity by Siva1. *Cell Death Differ* 16: 1493–1504.
19. Schulze E, Asai DJ, Bulinski JC, Kirschner M (1987) Posttranslational modification and microtubule stability. *J Cell Biol* 105:2167–2177.
20. Webster DR, Borisy GG (1989) Microtubules are acetylated in domains that turn over slowly. *J Cell Sci* 92:57–65.
21. le Gouvello S, Manceau V, Sobel A (1998) Serine 16 of stathmin as a cytosolic target for Ca2+/calmodulin-dependent kinase II after CD2 triggering of human T lymphocytes. *J Immunol* 161:1113–1122.
22. Beretta L, Dobránsky T, Sobel A (1993) Multiple phosphorylation of stathmin. Identification of four sites phosphorylated in intact cells and in vitro by cyclic AMP-dependent protein kinase and p34cdc2. *J Biol Chem* 268:20076–20084.
23. Rubin CI, Atweh GF (2004) The role of stathmin in the regulation of the cell cycle. *J Cell Biochem* 93:242–250.
24. Yano H, et al. (2004) Roles played by a subset of integrin signaling molecules in cadherin-based cell-cell adhesion. *J Cell Biol* 166:283–295.
25. Christofori G (2006) New signals from the invasive front. *Nature* 441:444–450.
26. Bershadsky A, Chausovsky A, Becker E, Lyubimova A, Geiger B (1996) Involvement of microtubules in the control of adhesion-dependent signal transduction. *Curr Biol* 6: 1279–1289.
27. Enomoto T (1996) Microtubule disruption induces the formation of actin stress fibers and focal adhesions in cultured cells: Possible involvement of the rho signal cascade. *Cell Struct Funct* 21:317–326.
28. Liu BP, Chrzanowska-Wodnicka M, Burridge K (1998) Microtubule depolymerization induces stress fibers, focal adhesions, and DNA synthesis via the GTP-binding protein Rho. *Cell Adhes Commun* 5:249–255.
29. Takahashi M, et al. (2002) Gene expression profiling of favorable histology Wilms tumors and its correlation with clinical features. *Cancer Res* 62:6598–6605.
30. Krylyshkina O, et al. (2002) Modulation of substrate adhesion dynamics via microtubule targeting requires kinesin-1. *J Cell Biol* 156:349–359.
31. Runge MS, Williams RC, Jr. (1982) Formation of an ATP-dependent microtubule-neurofilament complex in vitro. *Cold Spring Harb Symp Quant Biol* 46:483–493.
32. Vulevic B, Correia JJ (1997) Thermodynamic and structural analysis of microtubule assembly: The role of GTP hydrolysis. *Biophys J* 72:1357–1375.
33. Rosell R, et al. (2003) Transcripts in pretreatment biopsies from a three-arm randomized trial in metastatic non-small-cell lung cancer. *Oncogene* 22:3548–3553.
34. Minotti AM, Barlow SB, Cabral F (1991) Resistance to antimitotic drugs in Chinese hamster ovary cells correlates with changes in the level of polymerized tubulin. *J Biol Chem* 266:3987–3994.
35. Andersen JS, et al. (2002) Directed proteomic analysis of the human nucleolus. *Curr Biol* 12:1–11.
36. Daub H, Gevaert K, Vandekerckhove J, Sobel A, Hall A (2001) Rac/Cdc42 and p65PAK regulate the microtubule-destabilizing protein stathmin through phosphorylation at serine 16. *J Biol Chem* 276:1677–1680.